

# IBM Research Report

## Effects of Mechanical Deformation and Annealing on the Microstructure and Hardness of Pb-Free Solders

**Paul A. Lauro, Sung K. Kang, \*Won Kyoung Choi, Da-Yuan Shih**

IBM Research Division

Thomas J. Watson Research Center

P.O. Box 218

Yorktown Heights, NY 10598

\*Samsung Advanced Institute of Technology

P.O. Box 111, Suwon, 440-600, Korea



Research Division

Almaden - Austin - Beijing - Delhi - Haifa - India - T. J. Watson - Tokyo - Zurich

## Abstract

The microstructure-property relations of several Pb-free solders have been investigated in order to understand the microstructure changes during thermal and mechanical processes of Pb-free solder joints. Pb-free solder alloys investigated include pure Sn, Sn-0.7%Cu, Sn-3.5%Ag and Sn-3.8%Ag-0.7%Cu (in weight). To reproduce a typical microstructure observed in solder joints, the cooling rate, ingot size and reflow conditions of cast alloys are carefully controlled. The cast alloy pellets are subjected to compressive deformation up to 50% and annealing at 150°C, 48 h. The microstructure of Pb-free solders is evaluated as a function of alloy composition, plastic deformation and annealing. The changes in mechanical property are measured by microhardness test. The work hardening in Sn-base alloys is found to increase as the amount of alloying elements and/or deformation increases. The changes in microhardness upon deformation and annealing have been correlated with the microstructural changes, such as recrystallization or grain growth in Pb-free solder alloys.

**Key Words:** Pb-free solders, pure Sn, Sn-0.7%Cu, Sn-3.5%Ag, Sn-3.8%Ag-0.7%Cu, microstructure, compressive deformation, annealing, mechanical property, microhardness, recrystallization, grain growth.

## INTRODUCTION

Substantial progress has been made recently toward a full transition to lead (Pb)-free soldering technology owing to accelerated R & D efforts in industry, universities and national laboratories. Several promising lead-free solders to replace Pb-containing solders in microelectronic applications have been identified [1-13]. They include Sn-3.5Ag, Sn-0.7Cu, Sn-3.8Ag-0.7Cu, Sn-3.5Ag-4.8Bi, Sn-8Zn-3Bi, among others (in weight percent). These lead-free solders are all tin-rich with a melting point between 190°C and 227°C. They are recommended for various soldering applications, such as surface mount technology (SMT), plated-through-hole (PTH) joints, ball grid arrays (BGA), flip chip, and others. Despite the R & D progress and proliferation in published technical findings on Pb-free solders, our knowledge of these new solders is still at an infancy stage compared to Pb-containing solders. Especially, the fundamental questions on the microstructure-property relations in Pb-free solders, the microstructure evolution during thermomechanical processes, thermal fatigue mechanisms, creep and fatigue interactions, corrosion behavior of solder joints are not well answered yet.

In this study, the microstructure-property relations of several Pb-free solders have been investigated in order to understand the microstructure changes during thermal and mechanical processes of Pb-free solder joints. The microstructure of reflowed solder joints is mainly controlled by the solidification process of a molten solder. Hence, it is strongly influenced by the solidification conditions such as peak reflow temperature, cooling rate, solder volume, package or substrate size, and others. The resultant microstructure of solder joints is also influenced significantly by the nucleation and growth phenomena of constituent phases. The microstructure evolution in solder joints upon thermomechanical stressing is therefore even more difficult to predict since the complex interplays between the solidified microstructure and thermal/mechanical variables are expected.

In this study, the microstructure evolution of several Pb-free solder alloys has been investigated by applying thermal and mechanical variables independently. The strain hardening of each alloy is compared as a function of alloying elements as well as plastic deformation. The microstructural stability of the cast alloys is also studied.

## EXPERIMENTAL

Pb-free solder alloys investigated in this study include pure Sn, Sn-0.7Cu, Sn-3.5Ag, Sn-3.8Ag-0.7Cu (in weight %). A chill-cast ingot (approximately 88 mm x 17 mm x 12 mm) of each alloy composition was obtained commercially. To reproduce a typical microstructure observed in solder joints, the cooling rate, ingot size and reflow conditions of cast alloys were carefully controlled. A graphite mold having multiple cavities was employed to cast each solder alloy into a small pellet of 0.200" in diameter and 0.125" in height. After casting a molten solder into the graphite mold, solder pellets were reflowed at 260°C for 2 min, and solidified at a cooling rate of 3-4 °C/s. This cooling rate is somewhat higher than the typical cooling rate employed in a conventional reflow process, 0.5 to 1.5°C/s. Each cast alloy pellet was subjected to compressive deformation of 10, 20, 30 and 50%, respectively, in a MTS universal testing machine. To study the effect of heat treatment, as-cast and/or deformed solder pellets were subjected to an annealing treatment at 150°C, for 48 h, in a nitrogen gas. The microstructure of deformed solder pellets was examined on its cross section parallel to the direction of deformation by optical and SEM microscopy. To reveal the solder microstructure more clearly, the Sn matrix was lightly etched in a solution of 5% HNO<sub>3</sub>, 3% HCl, 92% CH<sub>3</sub>OH for several seconds. Microhardness tests were performed using 50 gf load on a cross section parallel to the direction of deformation in case of deformed samples. Vickers hardness number (HVN) was reported as an average value of 10 indentations or more.

## RESULTS

### Microstructure of As-cast Solders

Fig. 1 shows optical micrographs of a typical microstructure of as-cast alloys (top 4 micrographs) as well as the corresponding microstructure after annealing (150°C, 48 h) of each alloy (bottom 4). For pure Sn, a large grain structure is observed in as-cast condition, while further grain growth (or recrystallization) is noted in the annealed. For Sn-0.7Cu, Sn dendrites (light contrast) are dispersed uniformly in the matrix of Sn-Cu eutectic structure (dark contrast) in as-cast condition, while a recrystallized, large grain structure is noted in the annealed condition. For Sn-3.5Ag, Sn dendrites are

well developed along a certain direction in the matrix of Sn-Ag eutectic microstructure (dark contrast) in the as-cast condition, and some coarsening of Sn dendrites with random orientations is observed in the annealed. For Sn-3.8Ag-0.7Cu, Sn dendrites of irregular shapes are surrounded by Sn-Ag-Cu eutectic structure (dark contrast) in the as-cast condition, while further refining of Sn dendrites is noted in the annealed. Large, pro-eutectic  $Ag_3Sn$  plates, reported in Sn-Ag or Sn-Ag-Cu alloys solidified at a slow cooling rate [14], are not observed here in Sn-3.5Ag and Sn-3.8Ag-0.7Cu alloys as-cast or annealed, which were solidified at a relatively high cooling rate, 3-4°C/s.

### **Microstructure of Deformed Solders**

Fig. 2, 3 and 4 show a typical microstructure of four different alloys with a compressive deformation of 20%, 30% and 50%, respectively, (top 4). The annealed microstructure of each corresponding alloy upon heat treatment at 150°C, 48 h, is also shown in Fig.2, 3 and 4 (bottom 4). For pure Sn, there is no sign of the plastic deformation accumulated in the as-deformed condition, but a fully recrystallized microstructure for all level of deformation is noticed. Upon annealing of the deformed Sn, considerable grain growth occurs to produce a very large grain structure. For Sn-0.7Cu, the round Sn dendrite structure observed in the as-cast condition is significantly deformed according to the amount of plastic deformation. Upon annealing, the deformed microstructure has undergone a dramatic recrystallization process for each deformation level of 20%, 30%, and 50%. The resultant microstructure is quite different depending on the amount of deformation; the more deformation, the finer recrystallized microstructure. For Sn-3.5Ag, as the deformation increases, Sn dendrite structure is more squeezed and aligned. At the 50% deformation, the Sn dendrites are further refined and dispersed uniformly, as shown in Fig.4 (top 3rd). Upon annealing of Sn-3.5Ag at 150°C, the recrystallization is only observed in the solder deformed 30% or more. For Sn-3.8Ag-0.7Cu, the compressive deformation has also caused the dendrite structure to align and to be refined along the direction perpendicular to loading. Upon annealing, the grain growth is observed in the 20% deformed solder, while the recrystallization detected in the Sn-3.8Ag-0.7Cu solders deformed more than 30%.

## Microstructure of Deformed/Annealed Solders

Fig. 5 compares the microstructure of pure Sn as-cast, Fig.5 (left), with that of 50% deformed and annealed at 150°C, 48 h. In the as-cast condition, the microstructure of pure Sn has a grain size between 10 and 30  $\mu\text{m}$  (about 20  $\mu\text{m}$  in average). A Vickers' indentation mark shown in Fig.5 (left), corresponds to a microhardness number of about 8 (HVN). It is interesting to note the finer grain structure around the indentation mark, suggesting a possible recrystallization occurred at room temperature during indentation. Upon annealing at 150°C, followed by the plastic deformation of 50%, the pure Sn becomes a well-developed, large grain structure of an average grain size of 120  $\mu\text{m}$  or more, Fig.5 (right). This microstructure is attributed to the recrystallization process possibly during the deformation as well as further grain growth during the annealing.

Fig. 6 and 7 exhibit the microstructure evolution of Sn-3.8Ag-0.7Cu in the as-cast condition, Fig.6 (left), 30% deformed, Fig.6 (right), and deformed (30%)/annealed at 150°C, 48h, Fig.7 (right). Due to the compressive deformation of 30%, a significant refinement of Sn dendrite structure has been already made in the direction perpendicular to the deformation as shown in Fig.6 (right). Upon annealing at 150°C, 48 h, the deformed microstructure has undergone a recrystallization process to yield a finer microstructure of random orientation, Fig.7 (right), resembling to a “wrought” microstructure commonly observed in other alloy systems.

## Microhardness Measurement

Table I lists all microhardness results obtained in this study as a function of alloy composition, compressive deformation and annealing. They are also graphically shown in Fig.8. In general, the hardness of Sn-rich, Pb-free solders strongly depends on the alloying elements; the more alloying elements, the higher hardness. The plastic deformation to as-cast alloys has generally caused a strain hardening in each alloy, except in the pure Sn. This is consistent with the observation of the fully recrystallized microstructure in the pure Sn. The hardness of other deformed solders becomes substantially reduced upon annealing at 150°C, 48 h. The hardness reduction in the annealed solders is found to be more significant in the solders with more deformation. But, in the pure Sn, the hardness reduction upon annealing is not significant as in other solders. The hardness reduction in the

deformed/annealed solders generally reflects well the microstructure changes observed during the deformation and annealing processes.

## DISCUSSION

### Effects of Alloying Elements on Microstructure

The microstructure of Sn-rich solders is strongly influenced by the presence of alloying elements, such as Cu, Ag, or both. The dendritic growth morphology of the primary  $\beta$ -Sn crystal structure is unique in as-cast, Sn-0.7Cu, Sn-3.5Ag, and Sn-3.8Ag-0.7Cu alloys, while no dendritic structure is observed in the pure Sn solder either as cast or deformed. The binary eutectic microstructure either in Sn-0.7Cu or Sn-3.5Ag is a mixture of the intermetallic particles, either  $\text{Cu}_6\text{Sn}_5$  or  $\text{Ag}_3\text{Sn}$ , in the matrix of  $\beta$ -Sn phase. The ternary eutectic microstructure in Sn-3.8Ag-0.7Cu is a mixture of both  $\text{Cu}_6\text{Sn}_5$  and  $\text{Ag}_3\text{Sn}$  phases in the matrix of  $\beta$ -Sn. Both the binary and ternary eutectic structure are only observed in between the dendritic structure of primary  $\beta$ -Sn, suggesting the eutectic structure being solidified right after the  $\beta$ -Sn dendrite solidification. The volume fraction of the dendritic structure appears to decrease as the amount of alloying elements increases. Among the three alloys investigated, the volume fraction of the eutectic phase in the as-cast condition generally increases in order of Sn-0.7Cu, Sn-3.5Ag, and Sn-3.5Ag-0.7Cu, or roughly proportional to the total amount of the alloying elements added in the solders. The as-cast microstructure of the three solder alloys, solidified at the cooling rate of  $3.4^\circ\text{C}$  in this investigation, is simply characterized as a mixture of primary  $\beta$ -Sn dendrites and the eutectic phases. When a slow cooling rate is employed, the dendrite structure is expected to become coarser as reported previously [14, 15]. The coarse dendritic microstructure is also found to have a lower hardness value than the fast cooled, fine dendritic structure. Since the casting and solidification conditions used in this study are identical with the four solders examined, the difference in their microstructure is mainly attributed due to the alloying effects.

In addition, large pro-eutectic  $\text{Ag}_3\text{Sn}$  plates or  $\text{Cu}_6\text{Sn}_5$  rods were observed in the near ternary eutectic Sn-Ag-Cu alloys upon a slow cooling in the previous investigation [14, 15], but not in this study due to the relatively high cooling rate. The formation of the large pro-eutectic intermetallic phases in the binary or ternary alloys would cause a deviation in composition significantly from the eutectic

solidification, as well as in their microstructure. The propensity of forming the large intermetallics was explained by observing the large undercooling required for the  $\beta$ -Sn phase in the Sn-rich eutectic alloys [16]. In addition, the control of the large  $\text{Ag}_3\text{Sn}$  plates has been discussed by optimizing the composition of Sn-Ag-Cu alloys [15, 16].

### **Effects of Plastic Deformation on Microstructure and Hardening**

The compressive plastic deformation applied up to 50 % in height reduction has produced a progressive refinement of the dendrite structure in Sn-0.7Cu, Sn-3.5Ag, and Sn-3.8Ag-0.7Cu alloys, while no significant change is observed in the pure Sn. The microhardness measurements reflect well the strain hardening behaviors of pure Sn and Sn-rich alloys: more deformation yields a higher hardness value in Sn-rich alloys, but practically no hardening in the pure Sn.

The apparent no strain hardening is believed to be the recrystallization process occurred during the plastic deformation, which is discussed further in the next section. Since the pure Sn does not harden appreciably upon plastic deformation, the strain hardening of Sn-rich alloys can be understood mostly by the hardening of the eutectic microstructure in between the  $\beta$ -Sn dendrite arms. Hence, the volume fraction of the eutectic structure would be the key factor to determine the strain hardening behavior of Sn-rich solder alloys. As discussed earlier, since the volume fraction of the eutectic microstructure appears to increase as the amount of alloying elements, Ag, Cu, or both, the strain hardening of Sn-rich solders becomes more effective in the Sn-Ag-Cu over the binaries of Sn-Cu or Sn-Ag. This trend is clearly noted in Fig. 8, where the hardness variations are displayed as a function of alloying elements and plastic deformation. It is interesting to note when the plastic deformation is excessive, like 50% for Sn, Sn-0.7Cu and Sn-3.5Ag, the hardness of each alloy becomes lower than those of the smaller deformation. This may imply a microstructure change such as recrystallization has already occurred during the heavy plastic deformation of the alloys without any heat treatment.

### **Effects of Annealing: Grain Growth and Recrystallization**

The as-cast, Sn-rich solders, except for the pure Sn, are experiencing a considerable softening upon annealing at 150°C, 48 h, as shown in Table 1 and Fig. 8. From the microstructure study, in the annealed Sn-0.7Cu, the  $\beta$ -Sn dendrite structure has already changed into a large grain structure



possibly due to both the recrystallization and grain growth process, while in Sn-3.5Ag and Sn-3.5Ag-0.7Cu, the  $\beta$ -Sn dendrites are still persistent after the annealing, as noted in Fig. 1. This microstructure changes upon annealing appear to be consistent with the hardness changes shown in Fig. 8, where a very significant reduction in hardness is observed in the annealed Sn-0.7Cu, compared with Sn-3.5Ag or Sn-3.5Ag-0.7Cu. In the annealed Sn-3.5Ag and Sn-3.5Ag-0.7Cu, the hardness reduction becomes more pronounced in the solders with more deformation, as exhibited in Fig. 8. This suggests that for Sn-3.5Ag and Sn-3.5Ag-0.7Cu the recrystallization process requires both a considerable amount of plastic deformation, such as 30% or higher and the annealing condition such as 150°C, 48 h. In other words, the microstructural stability is much more with Sn-3.5Ag or Sn-3.5Ag-0.7Cu than Sn-0.7Cu or pure Sn. The resistance to the microstructural changes in these alloys can therefore be understood by the contribution of the uniform distribution of the eutectic microstructure and the  $\beta$ -Sn dendrites as well as the fine dispersion of intermetallic phases within the eutectic microstructure.

No appreciable strain hardening in the pure Sn is consistent with the microstructural observation of the plastically deformed Sn, where no significant changes in grain size is detected. This is possibly due to the recrystallization process occurred in the pure Sn during the plastic deformation at room temperature. In the literature, the recrystallization temperature of pure Sn is reported to be below room temperature, such as 25°F [17]. In the present investigation, we have observed small, recrystallized Sn grains along scratch lines during the mechanical polishing of the pure Sn samples, as well as during the microhardness indentation as shown in Fig. 5. The large grains of Sn shown in Fig. 5 after the annealing is therefore attributed to the grain growth of the recrystallized grains.

## CONCLUSIONS

Several Pb-free solder alloys have been investigated to understand the microstructure-property relations in terms of alloying composition, plastic deformation, and annealing condition. From this study, the following conclusions are drawn:

- 1). The microstructure of as-cast Sn-rich solder alloys is strongly influenced by the alloying elements, such as Cu, Ag, or both. The  $\beta$ -Sn dendrites are commonly observed in the binary or ternary Sn-rich alloys, but not in the pure Sn.
- 2). The microstructure of as-cast Sn-rich alloys is controlled by the solidification condition. At a fast cooling rate, the microstructure is composed of fine  $\beta$ -Sn dendrites surrounded by the binary or ternary eutectic structure. At a slow cooling rate, the coarse dendrites are mixed with the eutectic phase.
- 3). The strain hardening of Sn-rich solders is affected by the amount of alloying elements and plastic deformation. More plastic deformation yields a higher strain hardening. The more alloying elements, the higher strain hardening. However, the pure Sn does not show any appreciable hardening regardless of plastic deformation.
- 4). The recrystallization and (or) grain growth process have been observed in the deformed and annealed, Sn-rich solders depending on its plastic deformation or annealing condition. The pure Sn has undergone the recrystallization and grain growth at room temperature during plastic deformation, while in Sn-0.7Cu the recrystallization occurs after annealing at 150°C, 48 h, without any deformation.
- 5). For Sn-3.5Ag and Sn-3.5Ag-0.7Cu, the recrystallization requires both a considerable amount of plastic deformation, such as 30% or higher and the annealing condition such as 150°C, 48 h.

## **REFERENCES**

1. S. K. Kang and A. Sarkhel, *J. Elec. Materials*, 23(8), pp.701-7, (1994).
2. C.M. Miller, I.E. Anderson, and J.F. Smith, *J. Elec. Materials*, 23(7) (1994), pp.595-601.
3. P.T. Vianco, C. May, *Proc. Surface Mount Int. Conf*, pp.481-94 , (1995).
4. R. Ninomiya, K. Miyake, J. Matsunaga, *Proc. InterPACK'97*, p.1329, (1997).

5. "Lead-Free Solder Project Final Report," National Center for Manufacturing Sciences, Ann Arbor, MI, August (1997).
6. T. L. Ylikoki, H. Steen, A. Forsten, *IEEE Trans. Comp. Packg. & Manuf. Tech.*, Part C, 20(3), pp.194-198, (1997).
7. K. Habu, et al, *Proc.1997 7th IEEE Int. Symp. Elec.and Envir*, pp.21-24, (1999).
8. I.E. Anderson, et al., *J. Electronic Materials*, 30(9) (2001), pp.1050-1059.
9. D.R. Frear, J.W. Jang, J.K. Lin and C. Zhang, *JOM*, vol.53, No.6 (June 2001) p.28
10. S. K. Kang (ed.), "Lead-Free Solders," *JOM*, pp.16-41, June, (2001)
11. T. Taguchi, R. Kato, S. Akita, A. Okuno, H. Suzuki, T. Okuno, *Proc. 51<sup>st</sup> ECTC*, pp.675-680, May, (2001).
12. S. K. Kang, H. Mavoori, S. Chada, C. Kao, R. Smith (eds.), "Lead-Free Solder Materials & Soldering Technologies," *J. of Elec. Mat's*, 30(9), pp.1049-1270,(2001).
13. S. K. Kang (ed.), "Developments in Pb-Free Solders and Soldering Technology," *JOM*, pp.25-40, June, (2002).
14. D. W. Henderson, T. Gosselin, A. Sarkhel, S. K. Kang, W. K. Choi, D. Y. Shih, C. Goldsmith, K. J. Puttlitz, "Ag<sub>3</sub>Sn Plate Formation in the Solidification of Near Ternary Eutectic Sn-Ag-Cu Alloys," *J. Mater. Res.*, Vol.17, No.11, pp.2775-78, Nov, (2002).
15. S. K. Kang, W. K. Choi, D. Y. Shih, D. W. Henderson, T. Gosselin, A. Sarkhel, C. Goldsmith, K. J. Puttlitz, "Formation of Ag<sub>3</sub>Sn Plates in Sn-Ag-Cu Alloys and Optimization of Their Alloy Composition," *Proc. 53<sup>rd</sup> Electronic Components & Technology Conf*, New Orleans, LA, May 27-30, (2003).
16. D. W. Henderson, T. Gosselin, S. K. Kang, W. K. Choi, D. Y. Shih, C. Goldsmith, K. J. Puttlitz, "Lead-Free Tin-Silver-Copper Alloy Solder Composition," US Patent filed, February, 15, 2002.
17. A. Guy, *Elements of Physical Metallurgy*, Addison-Wesley Pub, Reading, MA, p.428, 1960.

**Table I. Microhardness of Pb-Free Solders as a Function of Deformation and Annealing**

<b>Alloy Composition (wt %)</b>	<b>Deformation % (st'd)</b>				<b>Annealing (150 ° C/48 h)</b>			
	<b>0 %</b>	<b>20 %</b>	<b>30 %</b>	<b>50 %</b>	<b>0 %</b>	<b>20 %</b>	<b>30 %</b>	<b>50 %</b>
<b>100 Sn</b>	<b>7.3 (0.10)</b>	<b>7.8 (0.14)</b>	<b>8.1 (0.41)</b>	<b>7.2 (0.27)</b>	<b>7.1 (0.42)</b>	<b>7.0 (0.37)</b>	<b>6.3 (0.71)</b>	<b>6.6 (0.67)</b>
<b>Sn-0.7Cu</b>	<b>11.1 (0.38)</b>	<b>12.5 (0.37)</b>	<b>13.4 (0.19)</b>	<b>12.6 (0.48)</b>	<b>8.1 (0.49)</b>	<b>8.5 (0.58)</b>	<b>8.6 (0.79)</b>	<b>9.1 (1.1)</b>
<b>Sn-3.5Ag</b>	<b>13.4 (0.30)</b>	<b>13.7 (0.52)</b>	<b>15.0 (0.77)</b>	<b>14.6 (0.30)</b>	<b>12.5 (0.74)</b>	<b>12.6 (0.64)</b>	<b>12.1 (0.65)</b>	<b>10.7 (0.97)</b>
<b>Sn-3.8Ag-0.7Cu</b>	<b>15.3 (0.55)</b>	<b>16.6 (0.61)</b>	<b>16.9 (0.53)</b>	<b>17.2 (0.73)</b>	<b>12.1 (0.43)</b>	<b>13.1 (0.82)</b>	<b>13.1 (0.87)</b>	<b>11.0 (0.78)</b>

# Grain Structure Change after Annealing

As Cast  
0% Deformation

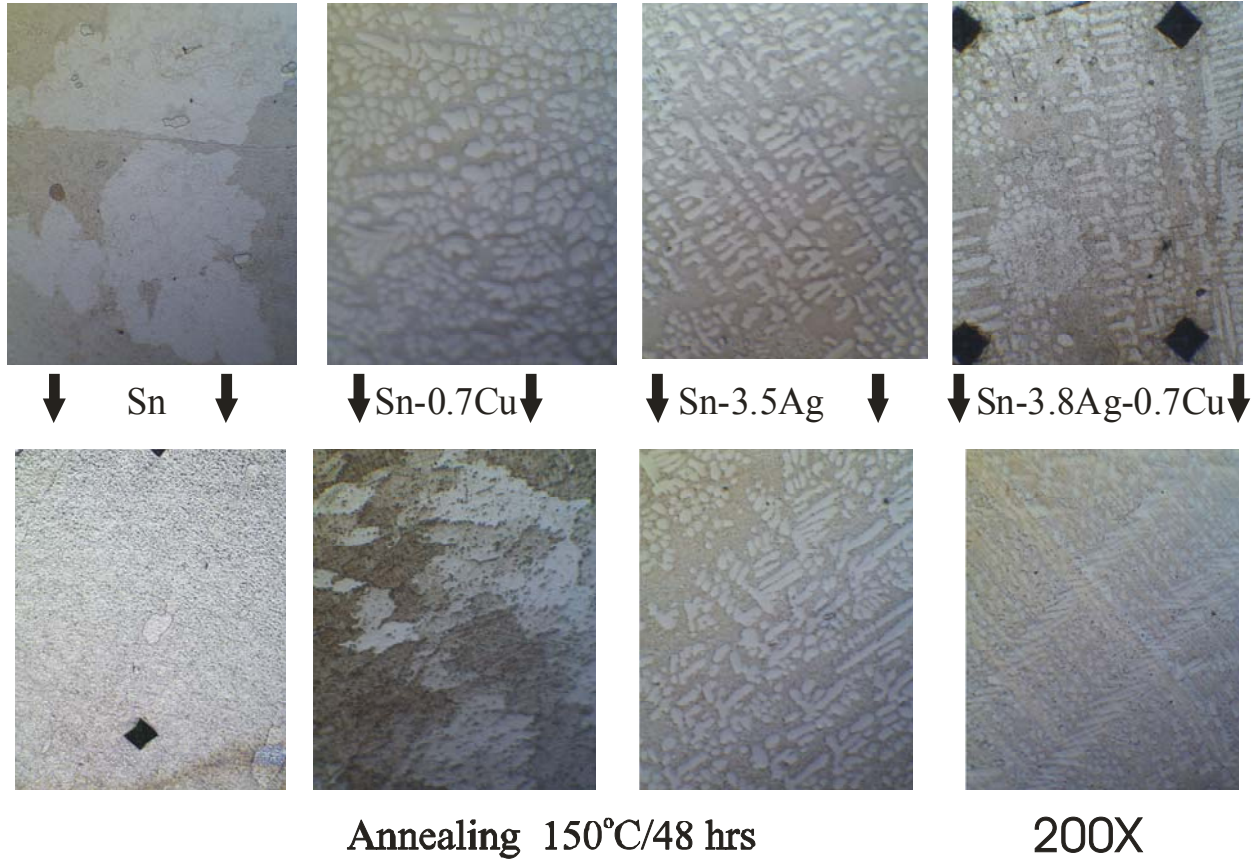


**Fig. 1. Optical micrographs of a typical microstructure of Sn and Sn-rich solder alloys in as-cast condition (top 4) and after annealing at 150°C, 48 h (bottom 4).**

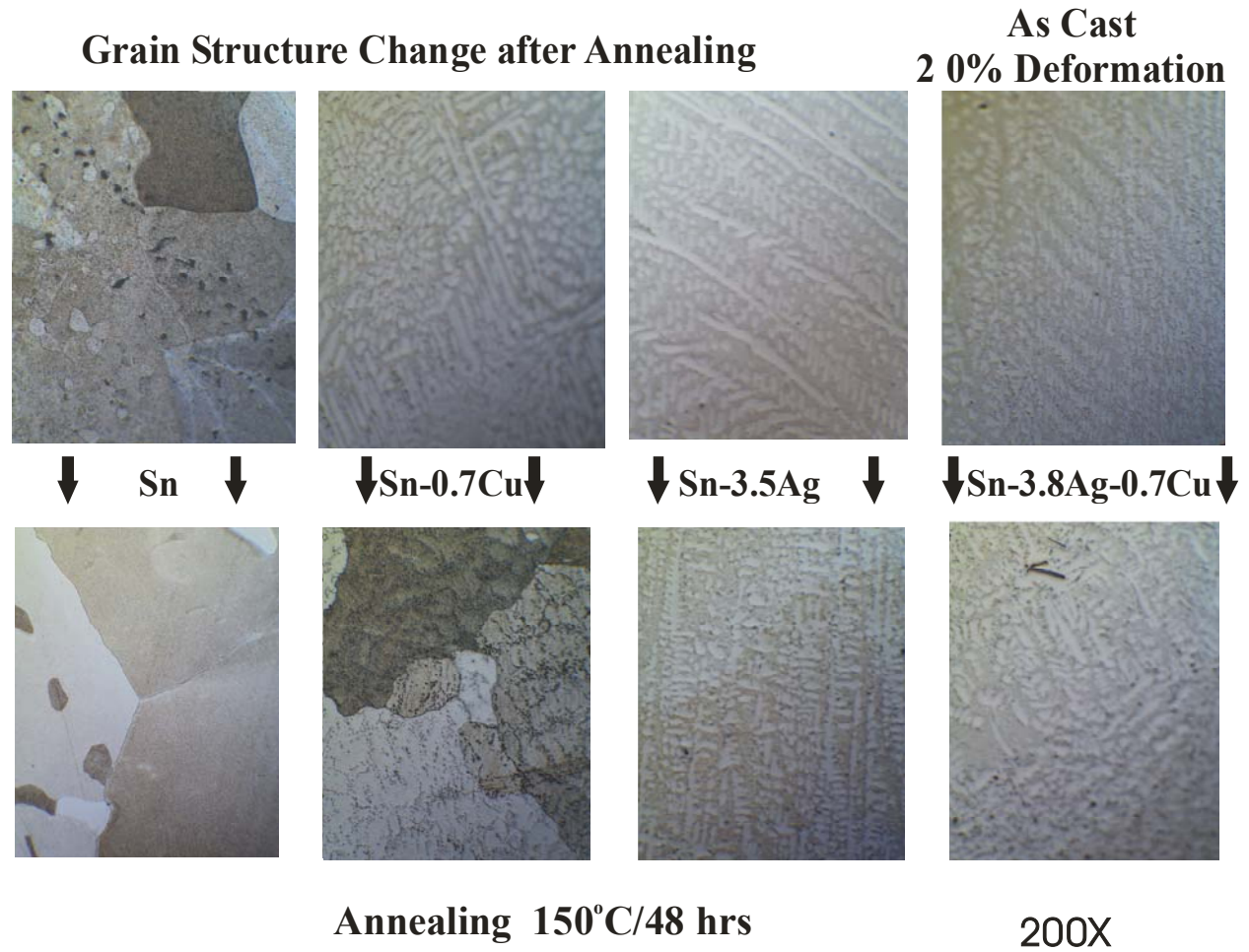


**Fig. 2. Optical micrographs of a typical microstructure of Sn and Sn-rich solder alloys 20% deformed (top 4) and annealed at 150°C, 48 h (bottom 4).**

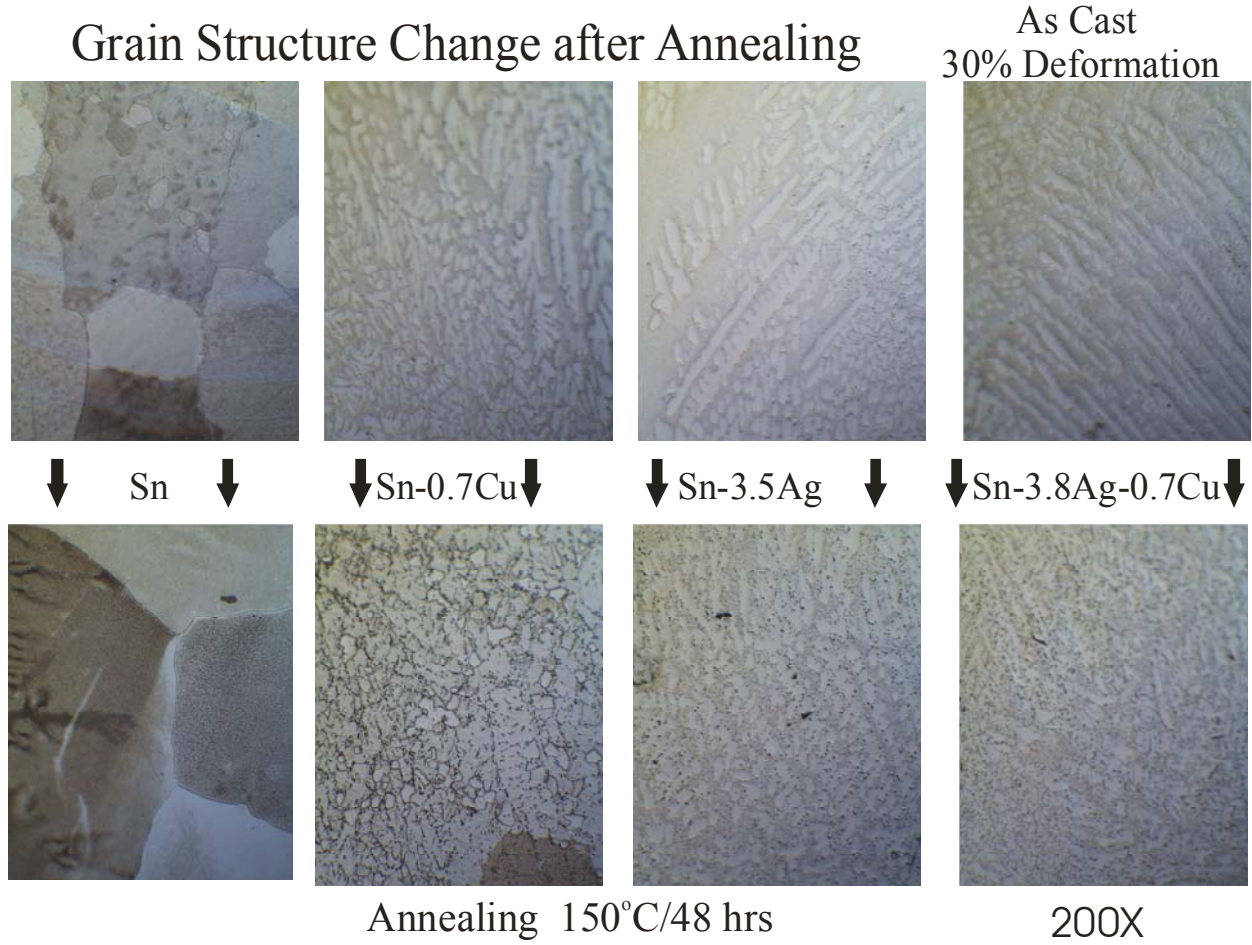


**Fig. 3. Optical micrographs of a typical microstructure of Sn and Sn-rich solder alloys 30% deformed (top 4) and annealed at 150°C, 48 h (bottom 4).**



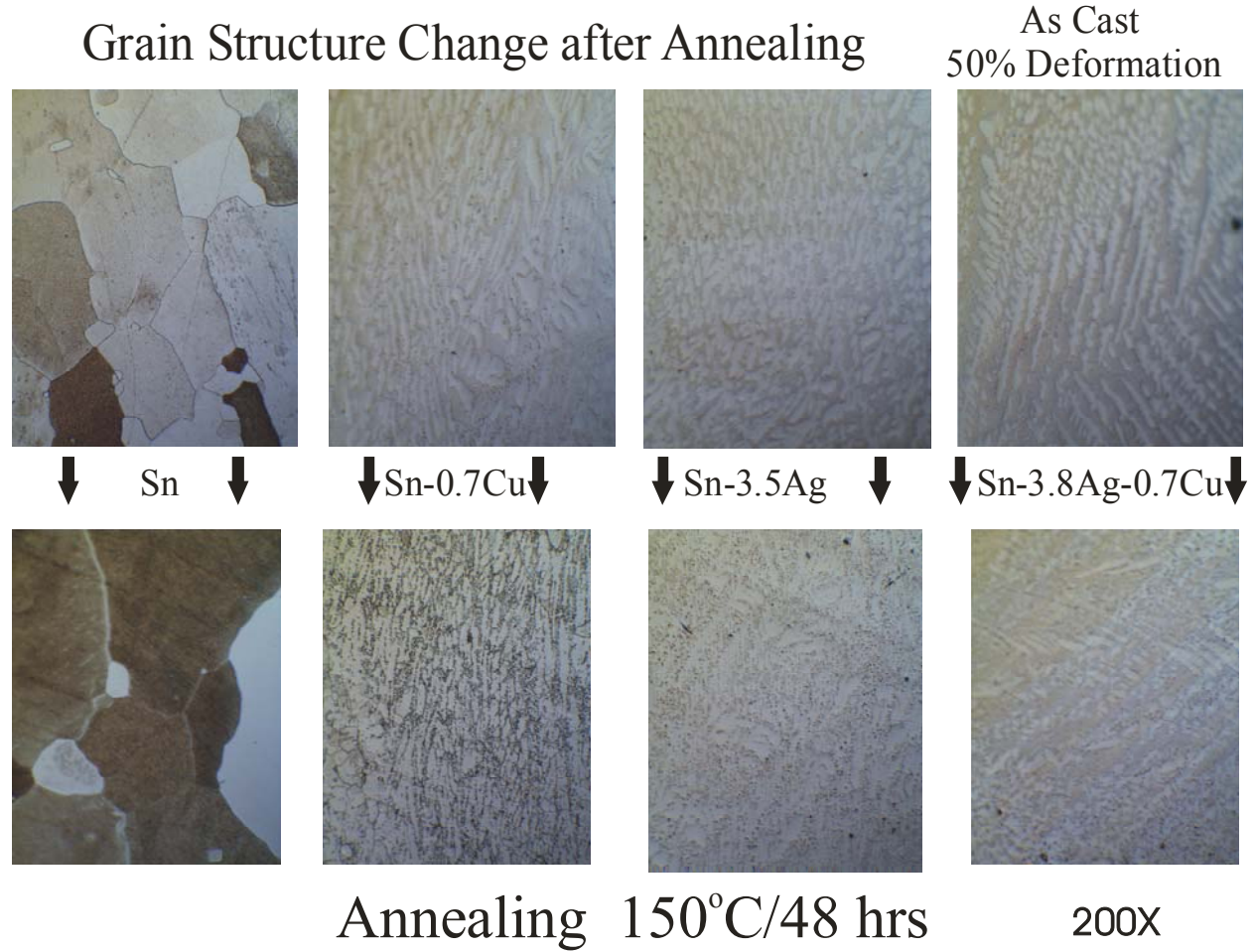


**Fig. 4. Optical micrographs of a typical microstructure of Sn and Sn-rich solder alloys 50% deformed (top 4) and annealed at 150°C, 48 h (bottom 4).**



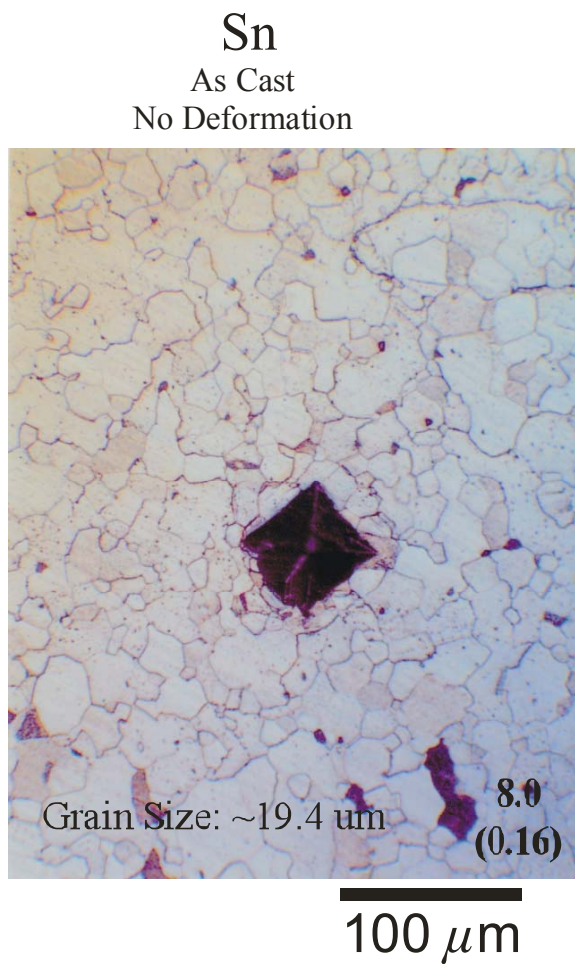


**Fig. 5. The microstructure of pure Sn as cast (left) and 50% deformed/annealed (right). The large grain structure in the deformed/annealed condition is attributed to recrystallization and grain growth.**

## Deformation Effect on Microstructure of Sn-3.8Ag-0.7Cu

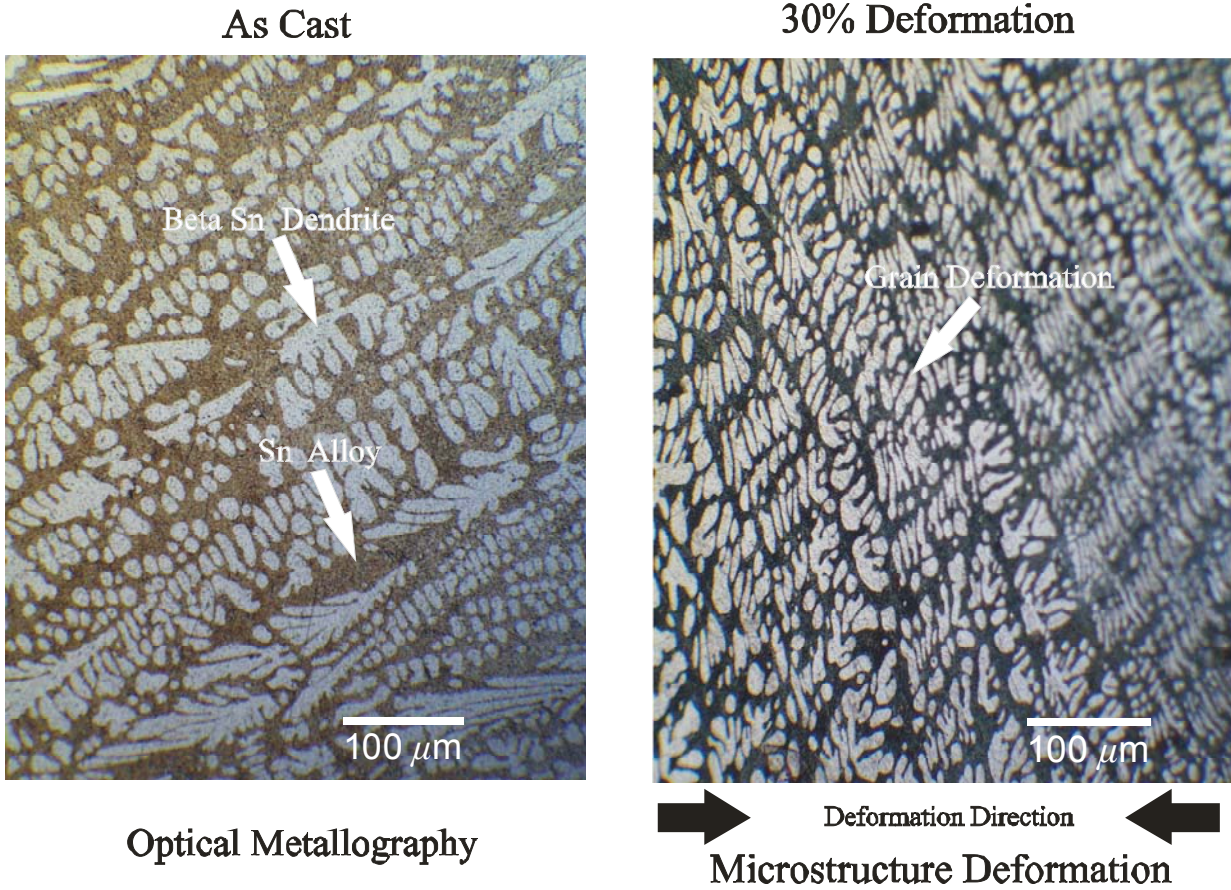


**Fig. 6. The microstructure of Sn-3.8Ag-0.7Cu as-cast (left) and 30% deformed (right). The direction of the plastic deformation is indicated by arrows (right).**



## Annealing Effect on Microstructure of Sn-3.8Ag-0.7Cu

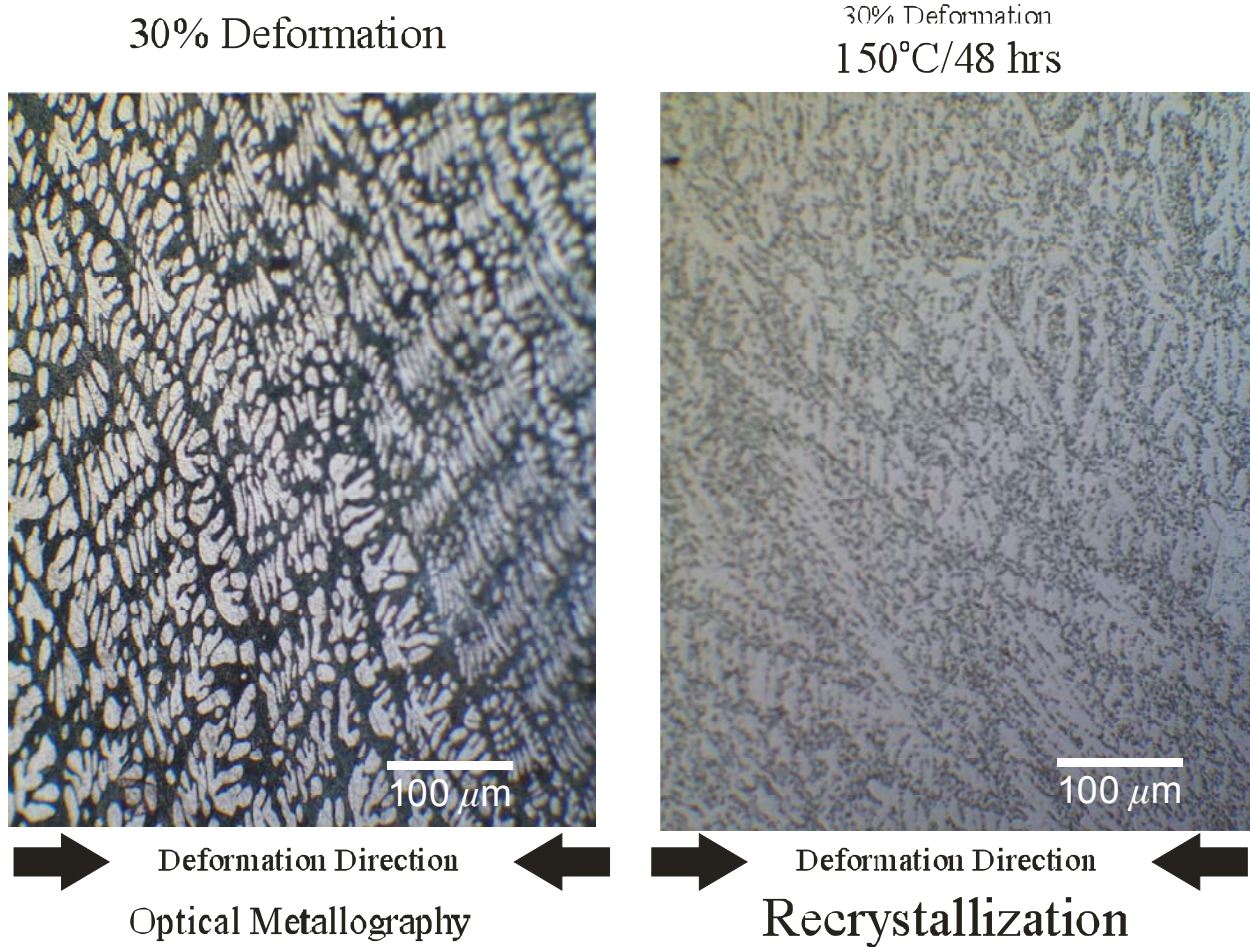


**Fig. 7. The microstructure of Sn-3.8Ag-0.7Cu deformed 30% (left) and annealed (right). The recrystallization is attributed to the microstructural change in the annealed.**

**Fig. 8.** The microhardness measurements of Sn and Sn-rich alloys as a function of alloy composition, plastic deformation and annealing. For each group, the hardness bars are arranged in order of the plastic deformation (0, 20, 30, and 50%).

